

AnalogSeeker: An Open-source Foundation Language Model for Analog Circuit Design

Zihao Chen[†], Ji Zhuang[†], Jinyi Shen, Xiaoyue Ke, Xinyi Yang,
Mingjie Zhou, Zhuoyao Du, Xu Yan, Zhouyang Wu, Zhenyu Xu, Jiangli Huang,
Li Shang *Member, IEEE*, Xuan Zeng *Senior Member, IEEE*, and Fan Yang* *Member, IEEE*

Abstract—In this paper, we propose *AnalogSeeker*, an effort toward an open-source foundation language model for analog circuit design, with the aim of integrating domain knowledge and giving design assistance. To overcome the scarcity of data in this field, we employ a corpus collection strategy based on the domain knowledge framework of analog circuits. High-quality, accessible textbooks across relevant subfields are systematically curated and cleaned into a textual domain corpus. To address the complexity of knowledge of analog circuits, we introduce a granular domain knowledge distillation method. Raw, unlabeled domain corpus is decomposed into typical, granular learning nodes, where a multi-agent framework distills implicit knowledge embedded in unstructured text into question-answer data pairs with detailed reasoning processes, yielding a fine-grained, learnable dataset for fine-tuning. To address the unexplored challenges in training analog circuit foundation models, we explore and share our training methods through both theoretical analysis and experimental validation. We finally establish a fine-tuning-centric training paradigm, customizing and implementing a neighborhood self-constrained supervised fine-tuning (NSC-SFT) algorithm. This approach enhances training outcomes by constraining the perturbation magnitude between the model’s output distributions before and after training. In practice, we train the Qwen2.5-32B-Instruct model to obtain AnalogSeeker, which achieves 85.04% accuracy on AMSBench-TQA, the analog circuit knowledge evaluation benchmark, with a 15.67% point improvement over the original model and is competitive with mainstream commercial models. Furthermore, AnalogSeeker also shows effectiveness in the downstream operational amplifier design task. These results suggest that AnalogSeeker acquires domain knowledge and has potential in giving design assistance. AnalogSeeker is open-sourced at <https://huggingface.co/analogllm/analogseeker> for research use.

Index Terms—analog circuit, electronic design automation, large language model, foundation model

I. INTRODUCTION

Analog circuits are characterized by a vast and sophisticated body of *knowledge*. Their wide range of functionalities, from basic modules such as operational amplifiers (opamps) and filters, to large-scale circuits such as phase-locked loops (PLLs) and analog-to-digital converters (ADCs), necessitates various design customizations to meet specific requirements. Despite this diversity, all analog circuits are rooted in esoteric and intricate theories, from the behavior of basic circuit components (such as resistors, capacitors, and transistors), to foundational circuit laws (such as Kirchhoff’s Current Law and

Kirchhoff’s Voltage Law). Such a unique blend of knowledge makes translating the analog circuit design process into fixed, programmable rules challenging. Therefore, existing electronic design automation (EDA) tools for analog circuits are limited and unable to fully support the varied applications or meet the demanding timelines.

Large language models (LLMs), like the GPT series [1]–[3], DeepSeek series [4], [5], and Qwen series [6]–[8], have recently shown remarkable capabilities in learning and applying human knowledge encoded in text. With billions of trainable parameters, the multi-head self-attention mechanism [9], and trillions of accessible training data, LLMs are adept at capturing long-range context dependencies and generating appropriate responses. Therefore, LLMs have already seen widespread adoption in many areas, most notably in software development [10]–[13], where the software community has a strong tradition of open-source collaboration and offers a vast amount of high-quality, accessible code data for training general-purpose LLMs as code experts.

However, general-purpose LLMs usually lack the knowledge of analog circuits, which hinders the potential of them to directly advance the automation of analog circuit design. For example, references [14] and [15] have demonstrated that, without further modification, many mainstream general-purpose LLMs cannot design even basic analog circuits.

Therefore, tailoring LLMs for specific analog circuit design tasks has been widely studied recently. For example, training LLMs on small, curated datasets has proven effective for designing specific circuits, such as opamps [14] and passive power converters [16]. On the other hand, multi-agent frameworks, equipped with chains of thoughts (CoTs) [17] and retrieval-augmented generation (RAG) [18], also empower general-purpose LLMs in analog circuit design [16], [19]–[21] without further training.

These works, relying on narrowly scoped, small-scale, human-curated datasets (or knowledge bases), offer notable advantages in both result effectiveness and design interpretability over traditional black-box optimization methods based on Bayesian Optimization (BO) [22]–[26] and reinforcement learning (RL) [27]–[30]. On the other hand, LLMs are demanded to conduct design operations based on restricted knowledge, without a full understanding of this domain.

Therefore, the motivation is suggested to explore a *foundation model* [31], [32] that could have the potential to learn the extensive knowledge of analog circuits. Such a model could serve as a foundation for developing general agents or as an

This work has been submitted to the IEEE for possible publication. Copyright may be transferred without notice, after which this version may no longer be accessible.

[†] These authors contributed equally to this paper.

* Corresponding author: yangfan@fudan.edu.cn.

initial step for further training in LLM-assisted analog circuit design, potentially supporting downstream tasks in the future.

However, we face the following significant challenges when building such a model:

Scarcity of data. Different from the software community, where open-source platforms like GitHub and Stack Overflow serve as rich data sources for LLM training, the analog circuit community is relatively niche and conservative, with few publicly accessible data resources available online. To date, progress in building analog circuit datasets has yet to explicitly target the extraction of textual domain knowledge. For example, the AMSNet series [33], [34] makes a commendable effort with labor-intensive manual annotation to transform visual data into text, and other initiatives such as [35] and [36] have made valuable contributions by focusing on the mapping between design variables and performance metrics for specific circuits like opamps. However, these approaches do not align closely with the needs of LLM training, which depends heavily on abundant natural language knowledge supervision. Thus, the challenge of collecting a large-scale, high-quality textual corpus that captures analog circuit knowledge remains both critical and unresolved.

Complexity of knowledge. Even if we obtain sufficient domain-specific corpus, it remains unstructured, unlabeled pre-training data. The hierarchical and coupled analog circuit knowledge still lies hidden within the raw text, awaiting extraction. From the perspective of breadth, this knowledge spans different learning stages and encompasses dozens of circuit types with vastly different principles and design considerations, ranging from basic filters and amplifiers to PLLs and ADCs. From the perspective of depth, each entry of knowledge may involve complex reasoning processes. For example, designing the transfer function of an opamp with Miller compensation involves multiple steps, from determining the structure to analyzing the transfer function, and deriving formulas for phase margin, bandwidth, and other parameters. Therefore, there is an urgent need to extract granular, well-structured knowledge entries from raw text to facilitate effective learning by LLMs.

Difficulty of training. Even with labeled data available, the overall training strategy and specific algorithms for LLM training remain unexplored. On the one hand, overall training strategies for LLMs often require customization for different domains. For example, in code generation scenarios, continual pre-training (CPT) [37] on massive code repositories is typically considered crucial [12], [13] before supervised fine-tuning (SFT) [38]. However, research in mathematics [39], [40] and chemistry [41] has found that SFT is the key determinant of model performance. On the other hand, how to customize specific training algorithms that can learn complex analog circuit knowledge as well as possible under the severely limited data scale, remains largely unexplored. Given the lack of precedent in this field, it is essential to carefully consider domain characteristics to identify a training method rather than replicating approaches from other fields.

This paper attempts to tackle these challenges and presents *AnalogSeeker*, an effort toward a foundation model for analog circuit design demanding extensive domain knowledge.

AnalogSeeker is open-sourced for academic research use at <https://huggingface.co/analogllm/analogseeker>.

Detailed contributions of this paper are listed as follows:

- A corpus collection method based on analog circuit domain knowledge framework is employed to overcome the data scarcity in this field. First, available, canonical textbooks are regarded as the data source. We integrate the learning road-map of this field to collect over ten textbooks spanning different learning stages, including circuit theory, analog circuit fundamentals, analog integrated circuit design, and advanced circuit topics. This corpus undergoes rigorous cleaning processes and ultimately serve as textual training corpus with high quality and good coverage.
- A granular domain knowledge distillation method is proposed to extract latent, complex knowledge into explicit question-answer pairs. First, we decompose the cleaned corpus into granular units, where each learning node represents an indivisible subsection of a textbook. For each learning node, a multi-agent framework is introduced to extract question-answer pairs. Considering that analog circuit knowledge typically involves complex thinking processes, we establish a quadruple data format encompassing *question-thinking-solution-answer* (QTSA). Finally, we conduct multiple rounds of sampling for each learning node, thereby generating the fine-tuning dataset.
- A fine-tuning-centric training paradigm with a neighborhood self-constrained SFT (NSC-SFT) algorithm is proposed to effectively inject domain knowledge into LLMs. We first establish the overall training paradigm centered on SFT of instruct models through theoretical analysis and experimental validation. Subsequently, we customize and implement the NSC-SFT method, where we not only consider making the target model’s output closer to the labels, but also introduces a soft self-constraint that ensures the target model’s output probability distribution remains as similar as possible to the original (reference) model. The trained model can thereby preserve the performance of the original model and learn domain knowledge better.

In the experiment, we conduct the training process based on Qwen2.5-32B-Instruct and obtain *AnalogSeeker*. On the AMSBench-TQA benchmark [42] for analog circuit knowledge evaluation, it achieves an accuracy of 85.04%, with an improvement of 15.67% points over the original model, and is competitive with mainstream general-purpose LLMs like DeepSeek-v3 and GPT-4o. It can also pass the opamp design task in [19]. Therefore, *AnalogSeeker* does integrate some domain knowledge and can give some design assistance.

The remainder of this paper is organized as follows. Section II introduces prior knowledge. Section III proposes our methods. Section IV presents the experimental results. Section V concludes this paper.

II. PRELIMINARIES

A. Continual Pre-training of LLMs

LLMs that have been trained on generic web-scale corpus can be further adapted by a self-supervised phase on unlabeled text. This procedure, called continual pre-training (CPT) [37],

specializes the model while retaining its general abilities. When the continued corpus is domain-specific, CPT can also be referred to as domain-adaptive pre-training (DAPT) [43].

Let $\mathcal{D}_{\text{CPT}} = \{x^{(k)}\}_{k=1}^{N_{\text{CPT}}}$ be the continued corpus, where each sequence $x^{(k)} = (x_1^{(k)}, \dots, x_{N_k}^{(k)})$ contains N_k tokens produced by the same tokenizer as the base model, thus ensuring vocabulary compatibility. For a decoder-only architecture such as Qwen series [6]–[8], we minimize the auto-regressive negative log-likelihood loss function:

$$\mathcal{L}_{\text{CPT}}(\theta) = - \sum_{k=1}^{N_{\text{CPT}}} \sum_{i=1}^{N_k} \log p_{\theta}(x_i^{(k)} | x_{<i}^{(k)}), \quad (1)$$

where θ denotes the trainable parameters in this model, $x_{<i}^{(k)}$ is the left context $(x_1^{(k)}, \dots, x_{i-1}^{(k)})$, and $P_{\theta}(\cdot|\cdot)$ is the conditional distribution over the vocabulary obtained via a softmax layer. Minimizing this cross-entropy objective continues the original pre-training regime without injecting task-specific bias.

B. Supervised Fine-tuning of LLMs

Supervised fine-tuning (SFT) [38] adapts a pre-trained model to the reasoning style required by specific downstream tasks using labeled examples (nowadays typically formatted as question-answer pairs).

Let $\mathcal{D}_{\text{SFT}} = \{(x^{(k)}, y^{(k)})\}_{k=1}^{N_{\text{SFT}}}$ be the labeled training set, where $x^{(k)} = (x_1^{(k)}, \dots, x_{N_k}^{(k)})$ denotes the k -th input sequence (question) with N_k tokens, and $y^{(k)} = (y_1^{(k)}, \dots, y_{L_k}^{(k)})$ denotes the corresponding target sequence (answer) with L_k tokens. A decoder-only language model with parameters θ is optimized by the following cross-entropy loss function:

$$\mathcal{L}_{\text{SFT}}(\theta) = - \sum_{k=1}^{N_{\text{SFT}}} \sum_{j=1}^{L_k} \log p_{\theta}(y_j^{(k)} | x^{(k)}, y_{<j}^{(k)}), \quad (2)$$

where θ denotes the trainable parameters in this model, $y_{<j}^{(k)}$ is the left context $(y_1^{(k)}, \dots, y_{j-1}^{(k)})$, and the inner term maximizes the probability of the j -th ground truth token conditioned on the complete input and all previously generated target tokens. Minimizing Eq. (2) aligns the model’s output logits with labeled values.

C. Categorization of LLMs from Training Aspects

From a training perspective, LLMs fall into three tiers:

(i) Base models. LLMs are first trained from random initialization with a purely auto-regressive objective like Eq. (1) in a corpus with billions to even trillions of tokens [1], [7], [44]. This pre-training imparts broad statistical knowledge, yet leaves the models mostly unaligned with human instructions, so they cannot reliably follow instructions or produce safe and truthful dialogue [1], [2]. Therefore, additional SFT and RL from human feedback (RLHF) [45] stages are typically required before final deployment.

(ii) Instruct models. SFT and RLHF are important and expensive stages in converting a pre-trained base model into a reliable conversational agent, i.e., an instruct model. This process depends on large, diverse, and meticulously curated instruction

and preference data pairs. For example, the Qwen2.5 series employs millions of SFT and RLHF data, trains for two epochs with sequences up to 32k tokens, and requires multi-week runs on thousands of GPUs [7]. Although reference [46] shows that roughly ten thousand carefully curated instruction–response pairs can align a model for everyday dialogue, such small-scale supervision still falls short of the performance attained by official models, especially on more demanding tasks.

(iii) Reasoning models. RL is recently added on top of instruct models to build high-performance reasoning models. When training a reasoning model, it could first be initialized with SFT as a cold start, and then refined online with Group Relative Policy Optimization (GRPO) [5]. This pipeline gives the model better math and coding performance, but requires millions of preference pairs, weeks of training on thousands of GPUs. However, the parameter landscape of a reasoning model is usually sparsely redundant and highly sensitive, making the model prone to collapse. Further fine-tuning sometimes triggers performance degradation [47], [48].

D. Typical LLM Domain Customization Pipeline

In academic settings, the conventional workflow typically begins with CPT to incorporate domain text, followed by SFT on instruction data. Due to its higher resource demands, RLHF is often excluded in academic research. The effectiveness of these stages varies significantly across different domains.

In programming tasks, for example, CPT is typically indispensable. Modern code models are usually exposed to billions to trillions of raw code tokens [12], [13]. Such large-scale pre-training yields substantial gains over models that rely on SFT alone, suggesting that language-agnostic syntax and cross-language identifier semantics should be absorbed during CPT.

In contrast, mathematics appears far less reliant on CPT. For example, reference [39] solely trains a 13B model on 5M question–answer pairs, and achieves good performance matching or outperforming code-pretrained models of similar size. Follow-up work [40] further shows that scaling SFT alone enables even a vanilla 7B model to close most of the remaining gap. These findings suggest that general-purpose models already encode latent mathematical structure, which can be effectively unlocked through sufficiently rich SFT.

These mixed outcomes suggest that the training strategy is highly domain-dependent.

III. PROPOSED APPROACHES

A. Overall Workflow

Fig. 1 presents the workflow of this paper. In Section III-B, high-quality analog circuit text is initially gathered through a domain knowledge framework-based corpus collection method, which is then decomposed into learning nodes and distilled into granular labeled fine-tuning data in Section III-C. A fine-tuning-centric training strategy is explored with the customized NSC-SFT training algorithm in Section III-D. Experiments demonstrate the performance of the trained model and the effectiveness of the proposed method. We also share both the model and the gained experience in practice.

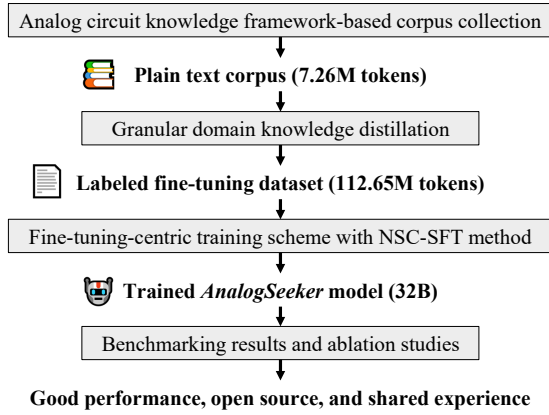


Fig. 1. The overall workflow and contribution of this paper.

B. Domain Knowledge Framework-based Corpus Collection

1) *Analog Circuit Knowledge Framework*: The discipline of analog circuits exhibits distinct hierarchical and progressive characteristics. The theoretical study of analog circuits is generally divided into four stages: circuit theory, analog circuit basis, analog integrated circuits, and advanced circuit topics. *Circuit theory* primarily encompasses basic circuit laws, network analysis methods, time and frequency domain analysis, and other fundamental knowledge, establishing the mathematical foundation for future learning. *Analog circuit basis* focuses on discrete device characteristics, basic amplifier circuits, feedback theory, and stability analysis, enabling learners to develop a fundamental understanding of circuit functionality and design methodologies. *Analog integrated circuits* delves into the design of core modules such as opamps, comparators, and reference circuits, as well as the implementation of circuits under CMOS technology. Finally, *advanced circuit topics* covers specialized circuits from opamps to PLLs.

2) *Corpus Collection and Processing*: Based on the aforementioned knowledge framework, we systematically collect canonical textbooks covering all learning stages. As shown in Table I Part 1, for the first three stages, we select several textbooks with complete content systems and accessible explanations, totaling 9 volumes. For the advanced circuit design stage, we select 11 reference books to cover core design methodologies in the major application domains. Ultimately, we construct a corpus containing 20 core textbooks legitimately for only academic use, which together span at least 12 major circuit types with overlaps, as detailed in Table I Part 2, from simple to complex.

At the implementation level, we employ the Mathpix commercial API for document processing, including text recognition, structured processing of mathematical formulas and tables, extraction and annotation of chapter hierarchy information, and desensitization and denoising. Consequently, we converted the original PDF files into a clean Markdown-formatted corpus totaling 7.26M tokens. While this corpus size remains relatively small and disadvantageous for training, it represents a valuable and hard-won resource.

TABLE I
DETAILS OF COLLECTED ANALOG CIRCUIT CORPUS

Part 1: Books Categorized by Learning Stage			
Learning stage	Circuit scope	Book Num.	
Circuit theory	Basic passive circuits	1	
Analog circuit basis	Basic amplifiers	3	
Analog integrated circuits	Various circuits	5	
Advanced circuits topics	Focused circuit(s)	11	

Part 2: Books Categorized by Circuit Types with Overlap			
Circuit type	Subtype Num.	Subtype example(s)	Book num.
Basic	-	-	4
Amplifier	6	Opamp, power amplifier	9
Arithmetic	4	Multiplier, divider	5
Filter	2	Active filter	6
Power management	2	DC-DC, AC-DC	2
Analog-to-Digital	8	SAR ADC, Σ - Δ ADC	6
Digital-to-Analog	2	Δ - Σ DAC	6
Reference	3	Voltage reference	5
Regulator	5	Linear regulator	5
Transceiver	4	Transmitter, modulator	5
Oscillator	3	VCO, LC oscillator	5
PLL	1	Charge-pump PLL	6

C. Granular Knowledge Distillation Method

In this section, we further investigate how to transform the unstructured, unlabeled corpus obtained in Section III-B into explicit, labeled data suitable for LLM training.

1) *Granular Decomposition of Corpus*: The cleaned corpus remains extremely long text files, making it difficult to effectively extract questions from it. A single book could cover different learning stages, encompassing dozens of circuits with vastly different principles and design considerations, ranging from basic filters and amplifiers to complex circuit systems.

To address this challenge, we first partition the cleaned corpus according to the extracted chapter and hierarchical information. We observe that analog circuit textbooks typically feature two-level subsections. For example, as shown in Fig. 2, a textbook related to circuit theory can usually be divided into many chapters, from *basic circuit components* to *frequency response of RLC filters*, each part being further subdivided into several subsections. We conduct statistics on the collected corpus and, after filtering out general introductory content, identify 2,698 valid subsections (or so-called *learning nodes*). We subsequently analyze the length of each subsection, finding an average of 2,002 tokens per subsection, which is a relatively moderate length, suitable for data distillation.

2) *QTSA Quadruple Data Format*: We aim to extract data from each learning node using LLMs. We note that each piece of knowledge within a data node may itself involve complex reasoning or problem-solving processes. For example, designing the transfer function of an opamp with Miller compensation, from architecture determination to analyzing the transfer function and deriving formulas for phase margin and bandwidth, involves multiple steps. Therefore, we adopt the following QTSA data format for each learning node $n(i)$:

$$\text{entry}(i) = [Q(i), T(i), S(i), A(i)], \quad (3)$$

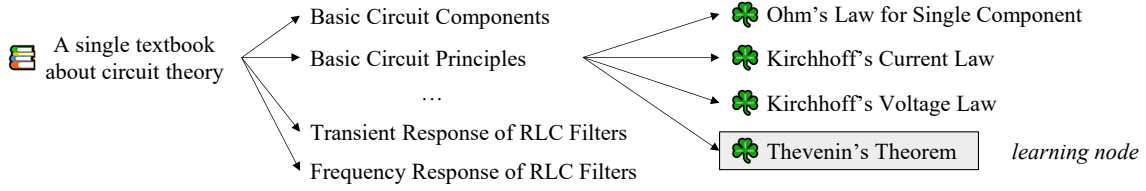


Fig. 2. An example of the granular decomposition of the cleaned corpus. From left to right, the granularity becomes progressively finer.

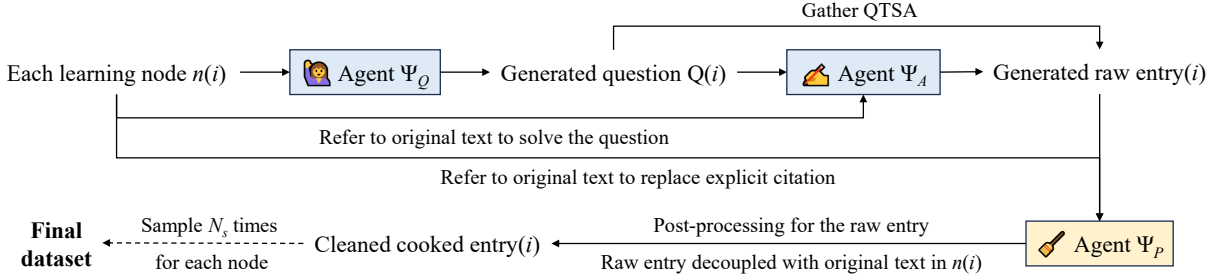


Fig. 3. The multi-agent framework for knowledge distillation. The upper half is the data generation stage, while the lower half is the post-processing stage.

where $Q(i)$ represents the generated question, $T(i)$ is the thinking process, which includes informal analysis of the problem as well as the entire process of formulating the final solution and answer, $S(i)$ is the refined and relatively structured solving process, and $A(i)$ is the final answer. Fig. 4 presents an easy example of the generated QTSA quadruple.

3) *Multi-agent Framework for Granular Knowledge Distillation*: Finally, we construct the multi-agent framework as shown in Fig. 3 to achieve granular knowledge distillation. For each node $n(i)$, agent Ψ_Q generates a question based on the given original content to obtain $Q(i)$:

$$Q(i) = \Psi_Q[n(i)]. \quad (4)$$

Subsequently, another agent Ψ_A refers to the original corpus $n(i)$ to answer the question, obtaining the thinking process, the solution method S , and the final answer, which are gathered as entry(i):

$$\text{entry}(i) = \Psi_A[n(i), Q(i)]. \quad (5)$$

As shown in Fig. 4, when we employ reasoning models like DeepSeek-R1 [5] that we adopt here, the model automatically generates $\langle \text{think} \rangle \dots \langle / \text{think} \rangle$ fields as the reasoning process during problem solving, naturally creating $T(i)$. The content outside the T field constitutes the solution process $S(i)$, and we specifically designate the final answer to be wrapped in the format $\langle \text{answer} \rangle \dots \langle / \text{answer} \rangle$ format. Furthermore, to ensure comprehensive knowledge coverage in each learning node, we independently sample each learning node for N_S times. In this paper, N_S is taken as 5.

The generated data undergoes further postprocessing and cleaning through the agent Ψ_P , which removes improperly formatted questions and corrects direct references to the content of the learning nodes (such as formula numbers and table numbers) in the original corpus, replacing them with specific content to decouple the data from the original corpus.

4) *Scale of the Final Dataset*: Table II presents the scale of the dataset we ultimately obtain. The original corpus was decomposed into 2.69k unlabeled CPT data, with a scale of

TABLE II
DETAILS OF COOKED ANALOG CIRCUIT DATASET

Training stage	Data piece num.	Data token num.
CPT	2.69k	7.26M
SFT	15.31k	112.65M

Question In a damped LC oscillator circuit with parallel resistance R , inductance L , capacitance C , and initial capacitor voltage $V_o = 1$ V. The switch closes at $t = 0$. The time for the oscillation amplitude to decay to 37% of its initial value is:
A) RC B) $1/(RC)$ C) $2/\omega_o$ D) $2RC$

Thinking $\langle \text{think} \rangle \dots$ We need to find the time for the oscillation amplitude to decay to 37% of its initial value. The oscillation amplitude decays exponentially with time. The amplitude falls to 37% of its initial value after a time equal to $2/\beta$. In the standard form of the differential equation:

$$\ddot{v} + \beta\dot{v} + \omega_o^2 v = 0,$$

where $\beta = 1/(RC)$. Thus, the time for the amplitude to decay to 37% is $2/\beta$:

$$T = 2/(1/(RC)) = 2RC.$$

\dots Why 37%? Because $1/e \approx 0.3679 \approx 37\%$, and the decay is as $e^{-\beta t/2}$ \dots The amplitude is: $V_o e^{-\beta t/2}$. Therefore $\dots \langle / \text{think} \rangle$

Solution The differential equation for the damped LC oscillator is \dots , where $\beta = 1/(RC)$ is the damping rate and $\omega_o = 1/\sqrt{LC}$ \dots The solution for the voltage is:

$$v = V_o e^{-\beta t/2} \left[\cos(\omega t) - \frac{\beta}{2\omega} \sin(\omega t) \right],$$

indicating the amplitude envelope decays exponentially as $V_o e^{-\beta t/2}$. To find when the amplitude decays to 37% of V_o , set $e^{-\beta t/2} = 0.37$. Since $1/e \approx 0.3679 \approx 37\%$, solve $e^{-\beta t/2} = e^{-1}$ gives:

$$-\beta t/2 = -1 \Rightarrow \frac{\beta t}{2} = 1 \Rightarrow t = \frac{2}{\beta}.$$

Substituting $\beta = 1/(RC)$ yields: $t = 2RC$. Thus \dots

Answer $\langle \text{answer} \rangle D \langle / \text{answer} \rangle$

Fig. 4. An easy example of QTSA data pairs. Some content details have been abbreviated using ellipses due to space limitations.

7.26M tokens. Using the multi-agent methods introduced in this chapter, we distilled 15.31k labeled data entries with 112.65M tokens. Although the scale is still limited compared to other fields, it is already a valuable training resource.

D. Customized Training Method for AnalogSeeker

1) *Model Selection for Training Initialization*: The selection of an appropriate pre-trained model as the initialization point is crucial for achieving an analog circuit LLM. As discussed in Section II-C, the current LLM landscape comprises three distinct categories, each of which presents unique characteristics that fundamentally impact their suitability for analog circuit knowledge learning.

(i) **Base models: impractical and unnecessary.** While base models offer theoretical flexibility for domain customization, we identify that adopting a base model is both impractical and unnecessary in our scenario. On the one hand, reproducing the instruction-tuning phase for base models is infeasible, since it requires the access to comprehensive SFT and RLHF datasets, which leading open-source models do not release [6]–[8]. On the other hand, high-quality instruct checkpoints like Qwen2.5-32B-Instruct are already publicly available, leaving expensive retraining from a base model unnecessary.

(ii) **Reasoning models: superior but fragile.** While reasoning models excel at complex tasks (a characteristic potentially advantageous for challenging analog circuit problems), we hypothesize according to Section II-C that their RL-heavy training methods compromises their adaptability to new domains. Specifically, the RL procedures create a highly specialized parameter manifold that, despite being optimal for reasoning tasks, exhibits extreme sensitivity to gradient perturbations during subsequent fine-tuning.

To empirically validate this hypothesis in the context of analog circuit design (a previously unexplored domain for this phenomenon), we conduct a controlled ablation study. As shown in Table III, fine-tuning QwQ-32B [7], a representative open-source reasoning model, results in a catastrophic performance degradation from 81.54% to 60.50% on the benchmark. This 21.04% decline not only confirms our theoretical prediction but also represents, to our knowledge, the first documented evidence of reasoning model fragility in the LLM domain customization for analog circuits.

(iii) **Instruct models: aligned and adaptable.** We identify instruct models as suitable initialization points for analog circuit LLM training. Theoretically, instruct models exhibit aligned but adaptable parameter spaces well-suited to analog circuit learning, which demands both precise context interpretation and adaptability to complex knowledge. In other words, while the RL-intensive training of reasoning models creates fragile parameter configurations, the SFT-focused alignment of instruct models preserves the flexibility needed to absorb the complex knowledge unique to analog circuits.

Empirically, fine-tuning Qwen2.5-32B-Instruct can achieve more than 15% performance improvements, validating that domain knowledge of analog circuits can be effectively integrated through the further training of existing instruct models.

2) *The SFT-centric Training Pipeline*: As discussed in Section II-D, domain adaptation typically employs both CPT and SFT. However, the optimal configuration remains domain-specific and requires careful investigation. Prior work suggests that CPT requires substantial data volumes typically exceeding 100M tokens [43]. Given our analog circuit corpus contains only 7.26M tokens for CPT (well below the recommended

threshold) versus 112.65M tokens for SFT (approximately 16× larger), we hypothesize that: CPT could provide minimal benefits due to insufficient data scale, while SFT alone may achieve comparable performance by directly teaching domain knowledge through instruction tuning.

To validate this hypothesis, we conduct a controlled ablation study in Section IV, comparing SFT-only versus CPT+SFT pipelines. Our results confirm that the CPT+SFT pipeline yields only a marginal 0.4% improvement over SFT alone (see Table III), which could be negligible and likely within the range of random variation. Therefore, an SFT-centric approach is more efficient for training an analog circuit LLM.

3) *Neighborhood Self-constrained SFT*: Because our domain-specific SFT dataset is costly yet limited (15.31k samples, 112.65M tokens), maximizing the utility of this dataset becomes important. An obvious observation in fine-tuning LLMs is that the adaptation process inevitably shifts the model’s semantic representation space [49], where SFT induces knowledge loss ΔK_{forget} (often called *forgetting* or *overfitting*) during the knowledge injection ΔK_{inject} process. For the sake of illustration only (not formal), the final gain of knowledge could be expressed as

$$\Delta K_{\text{gain}} = \Delta K_{\text{inject}} - \Delta K_{\text{forget}}. \quad (6)$$

Especially when the scale of the domain corpus is both small and difficult, the second term ΔK_{forget} could become non-negligible and could impact the performance because of training. Therefore, it becomes useful to mitigate the forget, i.e., to minimize ΔK_{forget} in order to maximize the overall knowledge gain ΔK_{gain} .

(i) **Proposal of NSC-SFT.** Mathematically, we hypothesize that it may be possible to construct a formulation in which, for any input x , the adapted model’s output probability distribution p_{predict} remains close to p_{ref} (the output probability distribution of the reference model before training) while still acquiring new knowledge. In doing so, the model could be encouraged to learn new knowledge without deviating significantly from its original behavior, thereby achieving anti-overfitting and potentially improving performance on the target domain. Similar intuition has been observed empirically in classical multi-task image classification [50] and RL [51], and has not been widely explored in the SFT of LLMs, particularly within specialized domains like analog circuit design automation. Therefore, we propose the following loss function:

$$\mathcal{L} = \mathcal{L}_{\text{CE}}(y_{\text{predict}}, y_{\text{label}}) + \lambda \cdot D_{\text{KL}}(p_{\text{predict}} \parallel p_{\text{ref}}), \quad (7)$$

where \mathcal{L}_{CE} is the standard cross-entropy loss in Eq. (2), measuring the discrepancy between the prediction y_{predict} and the label y_{label} ; λ is the weighting coefficient balancing the two objectives; and $D_{\text{KL}}(p_{\text{predict}} \parallel p_{\text{ref}})$ is the Kullback–Leibler (KL) divergence that gauges how far the current output distribution p_{predict} deviates from the reference distribution p_{ref} .

Moreover, we denote the trainable parameters of the current model and the reference model as θ and θ_0 , respectively:

$$D_{\text{KL}}(p_{\theta} \parallel p_{\theta_0}) = \sum_{v \in \mathcal{V}} p_{\theta}(v \mid x^{(k)}) \log \left[\frac{p_{\theta}(v \mid x^{(k)})}{p_{\theta_0}(v \mid x^{(k)})} \right], \quad (8)$$

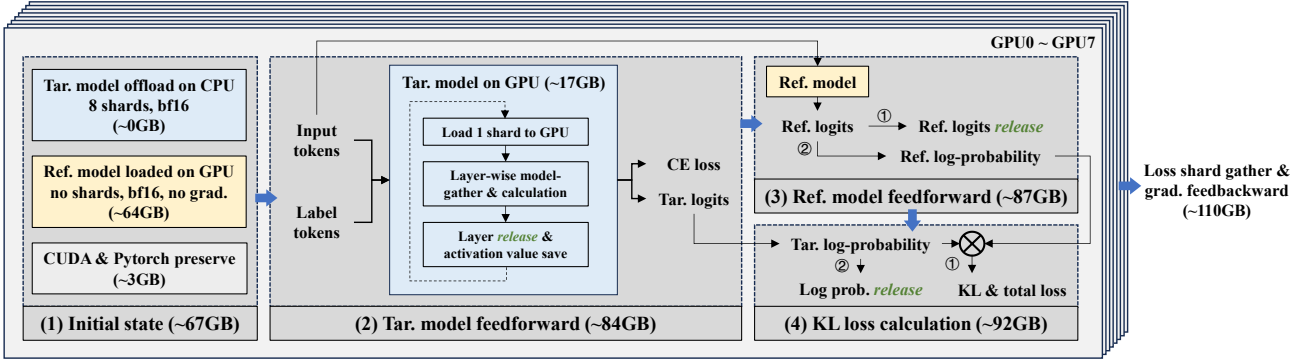


Fig. 5. The implementation of the proposed NSC-SFT algorithm. This diagram specifically demonstrates the data flow during the forward propagation and gradient backpropagation process, along with the theoretical estimates of the peak memory usage for each step.

where $v \in \mathcal{V}$ represents all possible tokens in the dictionary, $p_{\theta}(v | x^{(k)})$ is the output probability assigned by the current model to token v given input $x^{(k)}$, and $p_{\theta_0}(v | x^{(k)})$ is the output probability assigned by the reference model to the same token. This KL term, the *neighborhood self-constraint (NSC)*, ensures that the model remains close to its original semantic space while adapting to the analog circuit domain.

(ii) Convergence analysis of NSC-SFT. For completeness, we now prove the convergence of the NSC-SFT algorithm:

First, note that both the cross-entropy and KL divergence terms are smooth when the output distributions are bounded away from zero, which can be enforced by softmax and weight regularization. Therefore, the loss function $\mathcal{L}(\theta)$ is L -smooth, i.e., its gradient is Lipschitz continuous: for all θ, ϑ :

$$\|\nabla\mathcal{L}(\theta) - \nabla\mathcal{L}(\vartheta)\| \leq L\|\theta - \vartheta\|. \quad (9)$$

Second, note that the loss is non-negative: $\mathcal{L}(\theta) \geq 0$. This holds trivially, since both the negative log-likelihood and KL divergence are non-negative by definition.

Third, it is obvious that the learning rate η can be chosen in the standard range $\eta \in (0, 1/L)$.

Under these conditions, we can apply the standard descent lemma for L -smooth functions. After a gradient update $\theta_{t+1} = \theta_t - \eta\nabla\mathcal{L}(\theta_t)$, the loss satisfies:

$$\mathcal{L}(\theta_{t+1}) \leq \mathcal{L}(\theta_t) - \eta \left(1 - \frac{L\eta}{2}\right) \|\nabla\mathcal{L}(\theta_t)\|^2. \quad (10)$$

In particular, if $\eta < 1/L$, we obtain:

$$\mathcal{L}(\theta_{t+1}) \leq \mathcal{L}(\theta_t) - \frac{\eta}{2} \|\nabla\mathcal{L}(\theta_t)\|^2. \quad (11)$$

Summing inequality (11) from $t = 0$ to $T - 1$, we get:

$$\frac{\eta}{2} \sum_{t=0}^{T-1} \|\nabla\mathcal{L}(\theta_t)\|^2 \leq \mathcal{L}(\theta_0) - \mathcal{L}(\theta_T) \leq \mathcal{L}(\theta_0), \quad (12)$$

which shows that the gradient norms are square-summable, and hence $\|\nabla\mathcal{L}(\theta_t)\| \rightarrow 0$ as $t \rightarrow \infty$.

Note that $\mathcal{L}(\theta_t)$ is monotonically decreasing and lower bounded, and hence converges to some finite limit $\mathcal{L}_{\infty} \geq 0$. Since typical implementations employ weight decay or projection, the parameter sequence $\{\theta_t\}$ remains bounded.

In conclusion, under standard assumptions, the NSC-SFT algorithm generates a decreasing loss sequence to converge to a stationary point.

(iii) Implementation of NSC-SFT. Implementing NSC-SFT poses significant engineering challenges due to loading two very large models while managing KL divergence computation and gradient backpropagation. We present a practical implementation as illustrated in Fig. 5 to carefully manage memory usage and control computational load given the scarcity of available GPU resources, using a 32B model with an input token length of 8192 as the example.

First, we adopt an *asymmetric LLM memory management approach*. The target model (abbreviated as Tar. in Fig. 5) utilizes the DeepSpeed ZeRO-3 optimization method [52], partitioning parameters, gradients, and optimizer states across 8 GPUs, with each GPU storing only 1/8 of the model and offloading to the CPU most of the time. In contrast, we load the complete reference model (abbreviated as Ref. in Fig. 5) onto each GPU. Since the reference model does not participate in gradient backpropagation, the GPU memory usage from loading eight copies is acceptable. This approach also eliminates inter-GPU communication during reference model forward passes.

Second, we orchestrate the training process to manage memory peaks. From an initial ~ 87 GB (reference model and CUDA preserve), the target forward pass uses ZeRO-3's layer-wise strategy: For each layer, it performs an all-gather operation to reconstruct the complete layer parameters across GPUs, executes the forward computation, and immediately releases the gathered parameters back to CPU while preserving only the activation values. After CE loss calculation, we preserve only target logits and delete intermediate activations. The reference model then performs its forward pass locally on each GPU, bringing peak usage to ~ 87 GB. After that, both models' output logits must coexist briefly in memory, pushing usage to the training peak of ~ 92 GB. We compute KL divergence in log space using pre-computed log-softmax outputs, then delete both logit tensors before initiating the backward pass. The subsequent gradient computation expands memory usage to ~ 110 GB. Note that all memory usage figures above are rough theoretical estimates. In practice, owing to the memory pre-allocation and optimization mechanisms inside CUDA, the actual GPU memory allocation stabilizes at 101.37GB per device and confirms the efficacy of the proposed memory management strategy.

Other critical details include: BF16 precision loading for memory-accuracy balance; strict memory control with explicit tensor deletion at phase boundaries; and wrapping the reference model with fake quantization configuration to circumvent DeepSpeed’s restriction on loading different models with respective settings. These techniques collectively enable efficient NSC-SFT on standard hardware conditions with 8 devices.

IV. EXPERIMENTS

A. Basic Environment

1) *Hardware Environment*: We utilize a server with 8 NVIDIA H200 SXM GPUs, each equipped with 141GB memory (700W) and interconnected via NVLink, providing sufficient computational resources for medium-scale model training. For circuit simulation, we employ an Intel Xeon Platinum 8358 CPU featuring 128 cores operating at 2.60 GHz. All circuit implementations are based on TSMC 180-nm process technology.

2) *Software Environment*: Our software infrastructure is built on CUDA 12.2, ensuring compatibility with the Transformers framework [53] and DeepSpeed framework [52]. All models are trained using BF16 precision for memory efficiency, with flash-attention techniques [54], [55] disabled to maintain numerical stability during KL-divergence calculations. For inference and evaluation, we leverage vLLM [56] for high-throughput parallel processing.

B. Training Settings

1) *Model Choice*: The main training begins with Qwen 2.5-32B-Instruct, a medium-sized model that offers good baseline performance [7]. For ablation studies, we use the equally sized reasoning model QwQ-32B [57].

2) *General-Domain Data Mixing*: During the SFT phase, we incorporate the OpenThoughts dataset [58] with 20k samples alongside our analog-circuit domain data, maintaining a balanced scale between general and domain-specific samples.

3) *Hyper-parameter Settings*: We use a cosine-annealing scheduler with a 10% warm-up fraction, empirically determining that a maximum learning rate of 2×10^{-6} works well for both CPT and SFT, with modest variations showing negligible impact on performance. Our training configuration allocates 1 sequence per GPU batch with 8-step gradient accumulation, resulting in a global batch size of 64 that ensures training stability. We set the maximum sequence length at 8,192 tokens and implement packing for shorter sequences to maximize computational efficiency. Besides, the weighting coefficient λ in NSC-SFT is empirically set to 0.1.

C. Evaluation Settings

We evaluate our models using AMSBench-TQA (textual question-answering), a third-party benchmark in [42] designed by human experts for assessing LLM’s textual question-answering capabilities in analog circuit knowledge. which comprises a fixed set of multiple-choice problems, making automatic grading straightforward. All models share a system prompt to solve the question and give the final answer

TABLE III
PERFORMANCE COMPARISON OF DIFFERENT MODELS ON
AMSBENCH-TQA BENCHMARK

No.	Starting point	Method	Group	Acc. (%)
1	Qwen2.5-32B-Instruct	NSC-SFT	Exp.	85.04
2	Qwen2.5-32B-Instruct	CPT+NSC-SFT	Ctrl. II	84.49
3	DeepSeek-v3	—	Baseline	84.41
4	Qwen2.5-32B-Instruct	CPT+SFT	Ctrl. II	82.74
5	Qwen2.5-32B-Instruct	SFT	Ctrl. I	82.34
6	QwQ-32B	—	Baseline	81.54
7	QwQ-32B	SFT	Ctrl. III	74.94
8	GPT-4o	—	Baseline	73.99
9	Qwen2.5-32B-Instruct	CPT	Ctrl. II	71.20
10	Qwen2.5-32B-Instruct	—	Baseline	69.37

following a certain format, with a temperature value of 0. Additionally, we employ the Atelier framework [19] to validate if the model can assist opamp design.

D. Benchmarking Results and Analysis

Table III presents the performance comparison of various models on this benchmark. We comprehensively compare the proposed method with the most commonly used commercial LLMs including DeepSeek-v3 [4] and GPT-4o [3], the open-source baseline model Qwen2.5-32B-Instruct, and QwQ-32B, a reasoning model derived from Qwen2.5-32B-Instruct with a comparable scale.

1) *Comparison with Baseline Models*: As shown in Table III, the top-ranked model, referred to as the experimental group (abbreviated as *Exp.* in this table) and denoted as AnalogSeeker, is trained using the NSC-SFT method introduced in Section III-D. It achieves an accuracy of 85.04% on the benchmark, marking a 15.67% point improvement over the baseline instruct model Qwen2.5-32B-Instruct (69.37%) and reasoning model QwQ-32B (81.54%). Notably, it also outperforms two of the most widely used commercial models: DeepSeek-v3 (84.41%) and GPT-4o (73.99%).

This substantial gain clearly demonstrates the effectiveness of the comprehensive approach proposed in Section III, which includes corpus collection, data distillation, and model training strategies. By fine-tuning on the curated dataset, we successfully inject analog circuit knowledge into the model.

More specifically, DeepSeek-v3’s performance (84.41%) is comparable to ours. We attribute its strong performance primarily to its massive 671B parameter scale, the training corpus consisting of trillions of high-quality and diverse tokens (including many difficult math and code data) [4], both of which enable DeepSeek-v3 to encode rich knowledge and better reasoning abilities to earn a higher score on this benchmark.

On the other hand, GPT-4o’s relatively ordinary performance (73.99%) reflects its divergent training objectives. As GPT-4o is designed as a model for natural human-computer interaction, its training prioritizes versatility and broad applicability across diverse daily tasks [3] rather than deep knowledge in specific technical fields.

QwQ-32B’s performance (81.54%) is also good. Although QwQ-32B could lack the domain knowledge, its genuine reasoning capabilities acquired through RL [57] enable it to derive correct answers through logical deduction, thereby partially mitigating the limitations of domain knowledge and model scale. For example, as illustrated in Fig. 6, when analyzing noise in a classic CMOS opamp, QwQ-32B demonstrates its ability to apply basic formulas and reason through the problem, and finally recognizes that increasing g_{m1} reduces noise contribution from the first stage, and that reducing the g_{m3}/g_{m1} ratio increases first-stage gain, thereby lowering input-referred noise.

2) *Ablation Study I. Analysis of NSC-SFT*: The core innovation of NSC-SFT lies in introducing a KL divergence term that uses the original model as a reference, constraining the deviation of the model’s output distribution. As shown in Table III. The results of No. 1 and 5 models in control group I (abbreviated as *Ctrl. I* in this table) demonstrate the effectiveness of this design: Qwen2.5-32B-Instruct (NSC-SFT) achieves a 2.70% point improvement over Qwen2.5-32B-Instruct (SFT).

Fig. 6 provides a detailed example of this phenomenon. While Qwen2.5-32B-Instruct (NSC-SFT), i.e., AnalogSeeker, correctly analyzes CMOS opamp noise and selects the correct option, the SFT-only model, Qwen2.5-32B-Instruct (SFT), makes a critical error: it claims the g_{m3}/g_{m1} ratio only affects gain, not input-referred noise. This is fundamentally incorrect. In multi-stage opamps, the input-referred noise includes contributions from all stages, with later-stage noise referred to the input by dividing by the preceding gain. For a classical two-stage opamp where the first-stage gain is approximately g_{m1}/g_{m3} , the total input-referred noise becomes:

$$V_{n,in}^2 = V_{n1}^2 + V_{n3}^2 \cdot \left(\frac{g_{m3}}{g_{m1}}\right)^2, \quad (13)$$

where V_{n1}^2 and V_{n3}^2 are the noise power spectral densities of the first and second stages, g_{m1} and g_{m3} are the transconductances of the input and second-stage transistors. This equation clearly shows that increasing g_{m1}/g_{m3} reduces the second-stage noise contribution. The SFT-only model, (and most other models except DeepSeek-v3) fails to recognize this noise referral mechanism and claims exactly backwards.

This performance gain could be attributed to these factors: First, the KL constraint in Eq. (7) keeps parameter updates within a trust region near the original model, preventing the optimization from converging to poor local minima that may trap unconstrained SFT. Second, the constraint prevents overfitting to specific patterns in the training data, maintaining the model’s generalization ability on analog circuit questions. Rather than simply preventing knowledge loss, NSC-SFT could create a constrained optimization path that enables more effective integration of new domain knowledge while maintaining the pretrained model’s beneficial properties. This explains why NSC-SFT can successfully improve the performance of traditional SFT in our analog circuit case.

3) *Ablation Study II: Analysis of CPT*: The CPT phase should employ unsupervised domain texts for training, aiming to enhance the model’s understanding of analog circuit

<p>Question</p> <p>How can the input-referred noise voltage in a two-stage CMOS opamp be reduced? (A) Increasing the area (e.g., $W \times L$) and the g_m of transistors by adjusting W/L or current. (B) Reducing the g_{m3}/g_{m1} (g_{m4}/g_{m2}) ratio for load transistors. (C) Increasing the compensation capacitor C_c and drain current. (D) Both A and B are correct.</p>
<p>AnalogSeeker’s Response ✓</p> <p>...We need to consider the sources of noise and how they can be minimized. The input-referred noise voltage is primarily due to the noise generated by the input transistors (M_1 and M_2) and the load transistors (M_3 and M_4).</p> <p>Option A: Increasing the device area (W/L) of the input transistors (M_1 and M_2) can reduce the input-referred noise because the noise power is inversely proportional to the transconductance (g_m) of the input transistors. A higher g_m means a lower input-referred noise voltage...</p> <p>Option B: The noise from the load transistors (M_3 and M_4) can be reduced by decreasing the g_{m3}/g_{m1} (g_{m4}/g_{m2}) ratio. This is because the noise from the load transistors is referred to the input through the gain of the first stage. A lower g_{m3}/g_{m1} ratio means less noise from the load transistors is referred to the input.</p> <p>Option C: Increasing the compensation capacitor (C_c) and drain current is not directly related to reducing input-referred noise. These parameters are more related to stability and bandwidth of the opamp, not noise reduction.</p> <p>Option D: Both options A and B are correct as they both describe methods to reduce input-referred noise in a two-stage CMOS opamp. Therefore...</p>
<p>QwQ-32B’s Response ✓</p> <p>...Hmm, I need to recall what factors contribute to input-referred noise and how the different options affect that. First, input-referred noise in opamps generally comes from various sources like the input transistors (M_1 and M_2 in a differential pair), the load transistors (like M_3 and M_4), and maybe the second stage as well. Since it’s input-referred, we’re looking at noise sources that get amplified and then referred back to the input.</p> <p>Option A says increasing device area (like W/L) and increasing the g_m of transistors. Let me think. The transconductance g_m is proportional to the square root of the current and the W/L ratio. If you increase g_m, that would lower the noise because the noise voltage is inversely proportional to the gain. Wait, input-referred noise is the noise from each stage divided by the gain of the subsequent stages. So higher g_m in the first stage would mean that the noise from the first stage is divided by a higher gain, thus reducing its contribution. Also, increasing the device area (W/L) would increase g_m, so that makes sense.</p> <p>Option B suggests reducing the g_{m3}/g_{m1} ratio. The load transistors (M_3 and M_4) have their own noise. The g_{m3}/g_{m1} ratio is part of the gain of the first stage. The gain of the first stage is roughly $(g_{m1} + g_{m2}) \cdot (r_{o1} r_{o3})$, but the transconductance gain is $(g_{m1} \cdot r_{o3})$, where r_{o3} is the output resistance of M_3. The output resistance r_{o3} is $1/g_{m3}$. So the gain is g_{m1}/g_{m3}. So if you reduce the g_{m3}/g_{m1} ratio, that would mean increasing the gain of the first stage. Wait, because if g_{m3}/g_{m1} is smaller, then g_{m1}/g_{m3} is larger, so the gain is higher. So higher gain would mean that the noise from the first stage is divided by a higher gain, thus reducing input-referred noise. Wait, but the question is about the ratio of g_{m3}/g_{m1}. If you reduce that ratio (i.e., make g_{m3} smaller relative to g_{m1}), then the gain increases, which is good for reducing input-referred noise. So B might also be correct. But I need to be careful here...</p> <p>Option C says increasing the compensation capacitor and drain current. The compensation capacitor is part of the frequency compensation, which affects stability but not directly the noise. However, increasing the drain current would increase the transconductance there, which might lower the noise contribution from that stage. But the question is about input-referred noise, so maybe the second stage’s noise is referred back through the gain of the second stage? Not sure. But the compensation capacitor’s effect on noise isn’t obvious...</p> <p>Option D says both A and B are correct. Let me check again...</p> <p>For option A, increasing device area (W/L) of the input transistors would increase their g_m, which reduces their own noise (since noise voltage for a transistor is $\sqrt{4kT/I_D}$ something) and also the contribution is divided by the gain... So A’s first part (increase device area) and second part (increase g_m via W/L or current) both make sense. So A is a valid method.</p> <p>For option B, since the first stage gain is $(g_{m1})/(g_{m3})$, so lower ratio (g_{m3}/g_{m1}) means higher gain. So higher gain reduces the input-referred noise... So B is also correct.</p> <p>Therefore, both A and B are correct, so the answer would be D.</p>
<p>Qwen2.5-32B-Instruct (SFT) ✗</p> <p>To determine how to reduce the input-referred noise voltage in a two-stage CMOS opamp, we need to analyze the options provided and understand the underlying principles...</p> <p>Option A: The noise voltage of a transistor is inversely proportional to the square root of the device area. Therefore, increasing the device area (e.g., increasing W/L) reduces the noise voltage. Additionally, increasing the transconductance (g_m) of the transistors by adjusting W/L or the current also reduces the noise voltage because g_m is proportional to the square root of the current. This is because the noise voltage is inversely proportional to g_m. Therefore...</p> <p>Option B: This ratio is related to the gain of the opamp. Reducing this ratio would reduce the gain, which might not directly reduce the input-referred noise voltage. In fact, reducing the gain might increase the noise voltage because the noise voltage is inversely proportional to the gain. Therefore, this option is not correct.</p> <p>Option C: The compensation capacitor (C_c) is used to stabilize the opamp and does not directly affect the input-referred noise voltage. Increasing the drain current might increase the noise voltage because the noise voltage is proportional to the square root of the current...</p> <p>Option D: Both A and B are correct: Since option B is not correct... Based on the analysis, the correct option is A.</p>

Fig. 6. An example of models’ response to a question in the AMSBench-TQA benchmark. Note that for the same question, besides the model trained with NSC-SFT and the original QwQ-32B, DeepSeek-v3 also provides the correct answer, while most other models fail. Their logs are similar to those shown in this figure, and therefore, are not repeated here.

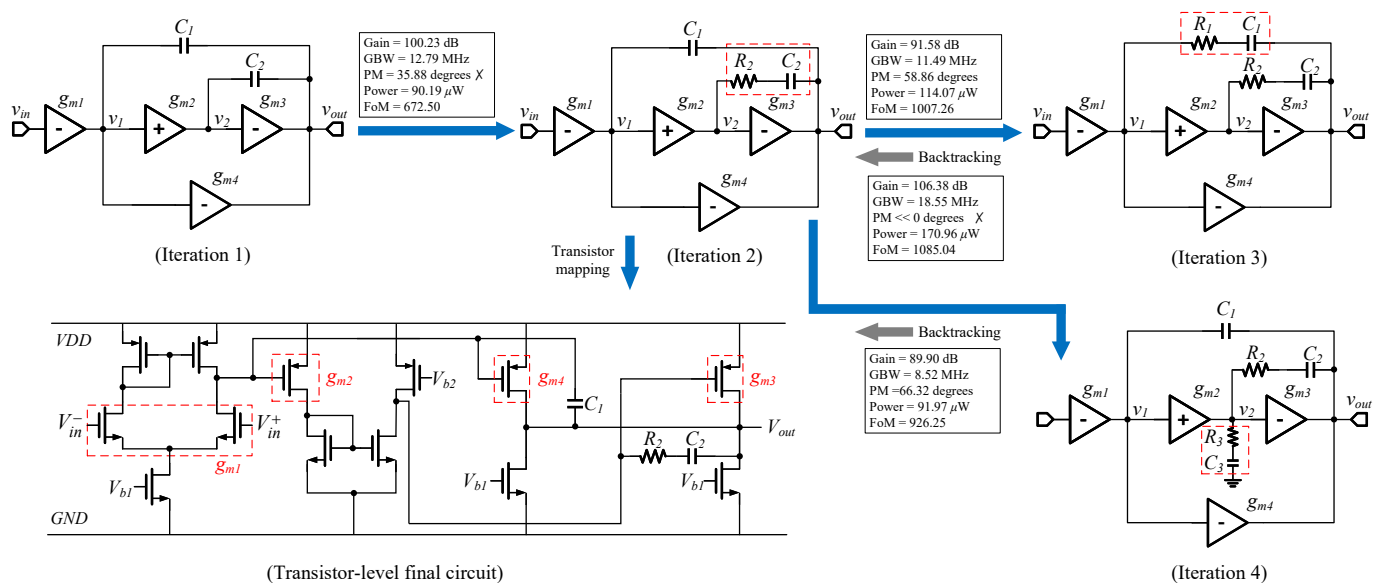


Fig. 7. The opamp design trajectory of the proposed AnalogSeeker under the Atelier framework. For each iteration, the circuit designed by the agent and its corresponding performance metrics are presented.

circuit domain language patterns without altering its conversational abilities. In Table III, Ctrl. II (No. 9 and 10 models) demonstrates that CPT alone yields a 1.83% performance improvement for Qwen2.5-32B-Instruct. However, our experiments reveal a critical limitation: after subsequent SFT, the benefits of CPT become negligible. For example, Qwen2.5-32B-Instruct (CPT+SFT) achieves only 0.4% higher accuracy than Qwen2.5-32B-Instruct (SFT). Moreover, compared to Qwen2.5-32B-Instruct (NSC-SFT), Qwen2.5-32B-Instruct (CPT + NSC-SFT) actually underperforms by 0.55%. These variations of approximately 0.5% could essentially be attributed to numerical random noise during the training process.

This phenomenon can be explained from two perspectives: From a data scale perspective, as shown in Table II, the CPT dataset is only 1/16 the size of the SFT dataset, resulting in a relatively limited impact on final model parameters. From a parameter update magnitude perspective, the supervised learning signal in the SFT phase is stronger, producing parameter updates far exceeding those from CPT, thereby overriding the subtle adjustments introduced by CPT.

4) *Ablation Study III: Analysis of Reasoning Models:* QwQ-32B, a reasoning-specialized model optimized through RL, exhibits a parameter distribution finely tuned for tackling complex reasoning tasks [57]. Consequently, as shown in Table III, it demonstrates remarkable performance on this analog circuit benchmark, outperforming GPT-4o by 7.55% even if the latter is significantly larger in scale. However, the results in Table III also reveal a trend: after SFT, Ctrl. III (No. 6 and 7 models) shows a notable performance drop of 6.60%.

This decline suggests that the reward signals utilized during RL training could have driven the model’s parameters into a highly specialized region of the parameter space, which could not be ideally aligned with domains required for further training. As a result, gradient descent struggles to find an optimal balance, i.e., one that both preserves the model’s

reasoning capabilities and adapts to new domains. Even though we employ a relatively low learning rate to mitigate excessive modifications to the original parameters, the model’s original capabilities are still hampered during training.

5) *Summary:* Based on the aforementioned analysis, our experiments lead to the following findings: (i) The NSC-SFT method, enhanced with appropriate KL regularization, outperforms traditional SFT in adapting to the domain of analog circuit knowledge. (ii) In the context of analog circuits, the imbalanced data distribution between the CPT and SFT stages makes direct SFT much more effective than CPT. (iii) Model selection is pivotal for achieving training success, with general instruct models proving to be more suitable as starting points for domain adaptation than highly specialized reasoning models. Despite the latter often demonstrating superior performance, their narrow specialization limits their adaptability to further training, thus making them less effective in domain adaptation. We hope that these experiences could help fellow researchers work on training analog circuit LLMs.

E. An Agent Case Study for AnalogSeeker

1) *Design Task Overview:* We attempt to use AnalogSeeker as agents in the classical opamp design framework Atelier, to evaluate whether it possesses the potential for design assistance. Specifically, within this task, the LLM directly undertakes three sub-tasks: topology design, topology modification, and circuit analysis. Topology design and modification refer to the process in which the agent designs or modifies the circuit topology based on current requirements or simulation results. Circuit analysis refers to the process in which the agent refines the topology into a SPICE netlist and lists the designable parameters and their ranges.

The detailed design trajectory is presented in Fig. 7, where the maximum number of iterations is set to 4 with a backtracking mechanism. More specifically, the detailed input and

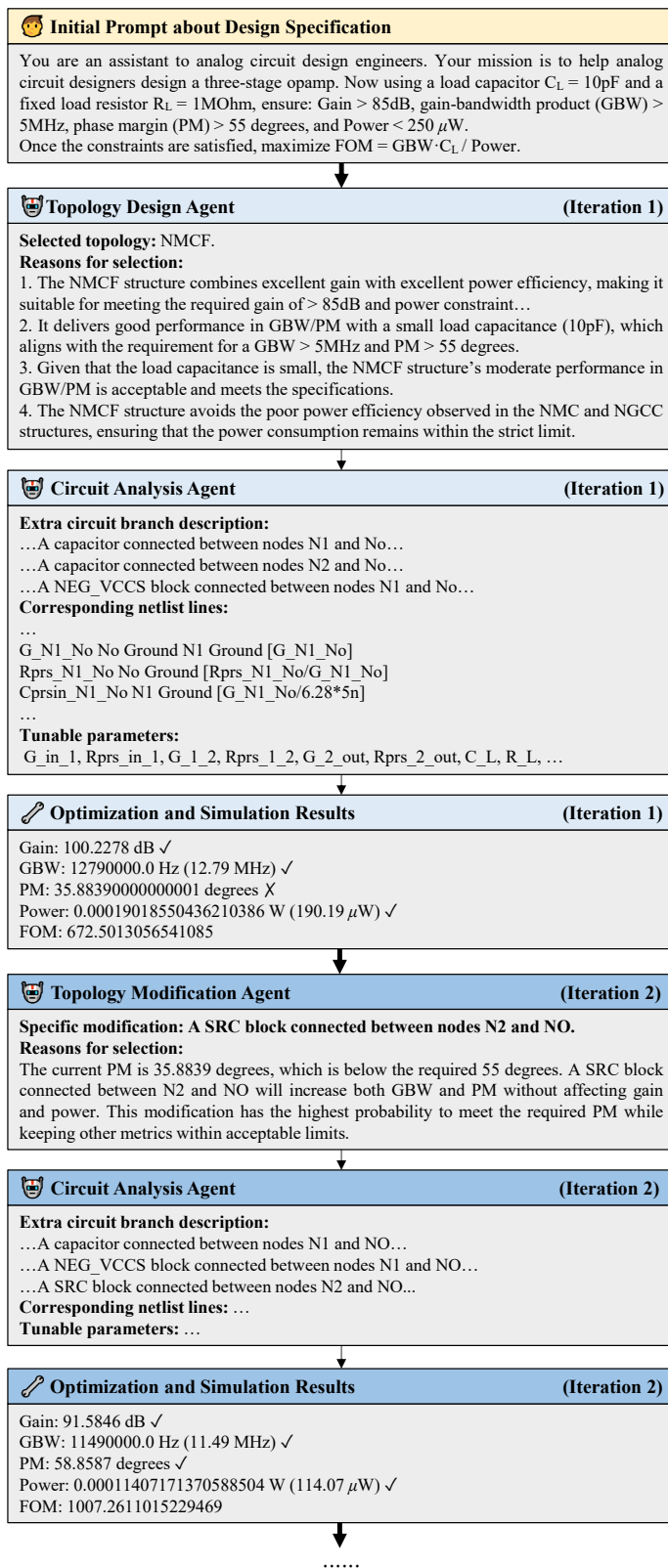


Fig. 8. The chatlog of AnalogSeeker within the Atelier opamp design framework. The model assumes the roles of two agents: a topology design/modification agent and a circuit analysis agent. The detailed dialogue of the first two iterations is shown here. Subsequent content is omitted, but the overall workflow can still be seen in Fig. 7. Besides, due to space limitations, some details of the content have been omitted using ellipses.

output content from the LLM during the first two design iterations is shown in Fig. 8, where we can also find the design specifications (specs) from the user's prompt. It can be observed that the agents' task is to maximize the Figure of Merits (FoM) while satisfying constraints on Gain, gain-bandwidth product (GBW), phase margin (PM), and power consumption. Among these, the requirement of GBW ($> 5\text{MHz}$) is challenging and could pose difficulty for the agent to achieve the stability of the designed circuit.

2) *Design Process Analysis:* As shown in both Fig. 7 and Fig. 8, in iteration 1, the topology design agent initially selects the NMCF (nested Miller compensation with feedforward) architecture as the starting design. This represents a rational decision, as NMCF achieves favorable stability (i.e., GBW/PM trade-off) while maintaining reasonable power consumption through its nested Miller compensation and feedforward paths [59], thus demonstrating potential to satisfy the design specs. The agent's topology selection and explanation in Fig. 8 align with these technical facts. Subsequently, the circuit analysis agent further refines the structural characteristics of the NMCF architecture into a SPICE netlist and systematically identifies the tunable parameters. Through classical BO sizing method [23], parameter optimization is conducted and performance metrics for the circuit are obtained. Notably, after the first iteration, the values of Gain, GBW, and Power meet the design specs, while PM = 35.88 degrees, indicating insufficient stability, which affects the basic functionality of this opamp.

In iteration 2, consequently, the topology design agent proposes introducing a series nulling resistor in addition to the Miller capacitor between the second stage and output stage (see both Fig. 7 and Fig. 8). It constitutes a useful approach, as the nulling resistor can further impede branch current flow, thereby enhancing circuit stability and phase margin. Following this modification, the second iteration design successfully satisfies all specs, with a good FoM value of 1107.26.

In iteration 3, to pursue enhanced circuit performance, the agent attempts to modify the outer loop to an RC series branch, aiming to further improve GBW, and consequently the FoM. Unfortunately, as shown in Fig. 7, while this modification does enhance GBW, it simultaneously results in a negative PM, rendering the circuit unstable. Therefore, the target design reverts to iteration 2.

In iteration 4, the agent further attempts to add a grounded RC branch to the second stage to improve FoM. This strategy successfully reduced power consumption from $114.07\ \mu\text{W}$ to $91.97\ \mu\text{W}$, but concurrently decreases GBW from 11.49MHz to 8.52MHz , resulting in a marginal reduction in overall FoM.

Therefore, the final selected design remains the iteration 2 version. The corresponding transistor-level circuit schematic is also presented in Fig. 7.

3) *Summary:* The aforementioned results provide preliminary evidence that AnalogSeeker can be successfully integrated into the Atelier framework to achieve opamp design, thus demonstrating nascent design assistance capabilities. Although these capabilities are constrained by the model's limited scale and relatively sparse training data, and may not significantly outperform commercial models, they nonetheless exhibit competitive potential.

V. CONCLUSIONS

In this paper, we have made an effort toward an analog circuit foundation model, developing *AnalogSeeker* and making it open-source for academic research use.

Specifically, we propose a domain knowledge framework-based corpus collection strategy to comprehensively gather high-quality classical textbooks available in the analog circuit domain, which are subsequently cleaned and processed into an unlabeled dataset containing 7.26M tokens. Through a granular knowledge distillation strategy, we further distill 112.65M tokens of fine-tuning data from the raw corpus to support model training. Customizing an NSC-SFT strategy with a feasible implementation approach, our trained model achieves a competitive score of 85.04% on the analog circuit knowledge evaluation benchmark AMSBench-TQA. Furthermore, the model demonstrates compatibility with the Atelier opamp design framework, exhibiting potential for giving some design assistance.

Additionally, this work presents extensive ablation studies and shares practical experience from our experimental process. Given the limited research budget and the challenges posed by data sparsity and learning difficulty inherent in this domain, we recommend that analog circuit LLMs adopt instruct models as the starting point, with fine-tuning as the core approach, and regularization techniques like NSC-SFT could further enhance training effectiveness.

This work will continue to be refined, and we plan to leverage larger-scale resources in the future to further enhance the model's capabilities. We hope this effort may provide some useful information to our research community.

ACKNOWLEDGMENTS

This research is supported by the National Natural Science Foundation of China (NSFC). We acknowledge the CFFF platform for providing computational resources that support our model training. This paper uses the generative AI including GPT series and Claude series only for grammar checking and readability improvement.

REFERENCES

- [1] L. Floridi and M. Chiriatti, "Gpt-3: Its nature, scope, limits, and consequences," *Minds and Machines*, vol. 30, pp. 681–694, 2020.
- [2] J. Achiam, S. Adler, S. Agarwal, L. Ahmad, I. Akkaya, F. L. Aleman, D. Almeida, J. Altschmidt, S. Altman, S. Anadkat *et al.*, "Gpt-4 technical report," *arXiv preprint arXiv:2303.08774*, 2023.
- [3] R. Islam and O. M. Moushi, "Gpt-4o: The cutting-edge advancement in multimodal llm," *Authorea Preprints*, 2024.
- [4] A. Liu, B. Feng, B. Xue, B. Wang, B. Wu, C. Lu, C. Zhao, C. Deng, C. Zhang, C. Ruan *et al.*, "Deepseek-v3 technical report," *arXiv preprint arXiv:2412.19437*, 2024.
- [5] D. Guo, D. Yang, H. Zhang, J. Song, R. Zhang, R. Xu, Q. Zhu, S. Ma, P. Wang, X. Bi *et al.*, "Deepseek-r1: Incentivizing reasoning capability in llms via reinforcement learning," *arXiv preprint arXiv:2501.12948*, 2025.
- [6] J. Bai, S. Bai, Y. Chu, Z. Cui, K. Dang, X. Deng, Y. Fan, W. Ge, Y. Han, F. Huang *et al.*, "Qwen technical report," *arXiv preprint arXiv:2309.16609*, 2023.
- [7] A. Yang, B. Yang, B. Zhang, B. Hui, B. Zheng, B. Yu, C. Li, D. Liu, F. Huang, H. Wei *et al.*, "Qwen2. 5 technical report," *arXiv preprint arXiv:2412.15115*, 2024.
- [8] A. Yang, A. Li, B. Yang, B. Zhang, B. Hui, B. Zheng, B. Yu, C. Gao, C. Huang, C. Lv *et al.*, "Qwen3 technical report," *arXiv preprint arXiv:2505.09388*, 2025.
- [9] A. Vaswani, N. Shazeer, N. Parmar, J. Uszkoreit, L. Jones, A. N. Gomez, Ł. Kaiser, and I. Polosukhin, "Attention is all you need," *Advances in neural information processing systems*, vol. 30, 2017.
- [10] D. Nam, A. Macvean, V. Hellendoorn, B. Vasilescu, and B. Myers, "Using an llm to help with code understanding," in *Proceedings of the IEEE/ACM 46th International Conference on Software Engineering*, 2024, pp. 1–13.
- [11] M. Wermelinger, "Using github copilot to solve simple programming problems," in *Proceedings of the 54th ACM Technical Symposium on Computer Science Education V. 1*, 2023, pp. 172–178.
- [12] B. Roziere, J. Gehring, F. Gloeckle, S. Sootla, I. Gat, X. E. Tan, Y. Adi, J. Liu, R. Sauvestre, T. Remez *et al.*, "Code llama: Open foundation models for code," *arXiv preprint arXiv:2308.12950*, 2023.
- [13] Z. Feng, D. Guo, D. Tang, N. Duan, X. Feng, M. Gong, L. Shou, B. Qin, T. Liu, D. Jiang *et al.*, "Codebert: A pre-trained model for programming and natural languages," *arXiv preprint arXiv:2002.08155*, 2020.
- [14] Z. Chen, J. Huang, Y. Liu, F. Yang, L. Shang, D. Zhou, and X. Zeng, "Artisan: Automated operational amplifier design via domain-specific large language model," in *2024 61th ACM/IEEE Design Automation Conference (DAC)*, 2024, pp. 1–6.
- [15] C.-C. Chang, Y. Shen, S. Fan, J. Li, S. Zhang, N. Cao, Y. Chen, and X. Zhang, "LaMAGIC: Language-model-based topology generation for analog integrated circuits," in *Proceedings of the 41st International Conference on Machine Learning*, 2024, pp. 6253–6262.
- [16] D. V. Kochar, H. Wang, A. Chandrakasan, and X. Zhang, "Ledro: Llm-enhanced design space reduction and optimization for analog circuits," *arXiv preprint arXiv:2411.12930*, 2024.
- [17] J. Wei, X. Wang, D. Schuurmans, M. Bosma, F. Xia, E. Chi, Q. V. Le, D. Zhou *et al.*, "Chain-of-thought prompting elicits reasoning in large language models," *Advances in neural information processing systems*, vol. 35, pp. 24 824–24 837, 2022.
- [18] P. Lewis, E. Perez, A. Piktus, F. Petroni, V. Karpukhin, N. Goyal, H. Küttler, M. Lewis, W.-t. Yih, T. Rocktäschel *et al.*, "Retrieval-augmented generation for knowledge-intensive nlp tasks," *Advances in Neural Information Processing Systems*, vol. 33, pp. 9459–9474, 2020.
- [19] J. Shen, Z. Chen, J. Zhuang, J. Huang, F. Yang, L. Shang, Z. Bi, C. Yan, D. Zhou, and X. Zeng, "Atelier: An automated analog circuit design framework via multiple large language model-based agents," *IEEE Transactions on Computer-Aided Design of Integrated Circuits and Systems*, 2025.
- [20] C. Liu, W. Chen, A. Peng, Y. Du, L. Du, and J. Yang, "Ampagent: An llm-based multi-agent system for multi-stage amplifier schematic design from literature for process and performance porting," *arXiv preprint arXiv:2409.14739*, 2024.
- [21] H. Zhang, S. Sun, Y. Lin, R. Wang, and J. Bian, "Analogxpert: Automating analog topology synthesis by incorporating circuit design expertise into large language models," *arXiv preprint arXiv:2412.19824*, 2024.
- [22] W. Lyu, P. Xue, F. Yang, C. Yan, Z. Hong, X. Zeng, and D. Zhou, "An efficient bayesian optimization approach for automated optimization of analog circuits," *IEEE Transactions on Circuits and Systems I: Regular Papers*, vol. 65, no. 6, pp. 1954–1967, 2017.
- [23] W. Lyu, F. Yang, C. Yan, D. Zhou, and X. Zeng, "Batch bayesian optimization via multi-objective acquisition ensemble for automated analog circuit design," in *International conference on machine learning*. PMLR, 2018, pp. 3306–3314.
- [24] J. Lu, L. Lei, F. Yang, C. Yan, and X. Zeng, "Automated compensation scheme design for operational amplifier via bayesian optimization," in *2021 58th ACM/IEEE Design Automation Conference (DAC)*. IEEE, 2021, pp. 517–522.
- [25] J. Lu, L. Lei, F. Yang, L. Shang, and X. Zeng, "Topology optimization of operational amplifier in continuous space via graph embedding," in *2022 Design, Automation & Test in Europe Conference & Exhibition (DATE)*. IEEE, 2022, pp. 142–147.
- [26] J. Lu, L. Lei, J. Huang, F. Yang, L. Shang, and X. Zeng, "Automatic op-amp generation from specification to layout," *IEEE Transactions on Computer-Aided Design of Integrated Circuits and Systems*, 2023.
- [27] H. Wang, K. Wang, J. Yang, L. Shen, N. Sun, H.-S. Lee, and S. Han, "Gcn-rl circuit designer: Transferable transistor sizing with graph neural networks and reinforcement learning," in *2020 57th ACM/IEEE Design Automation Conference (DAC)*. IEEE, 2020, pp. 1–6.
- [28] Z. Zhao and L. Zhang, "Analog integrated circuit topology ayntesis with deep reinforcement learning," *IEEE Transactions on Computer-Aided Design of Integrated Circuits and Systems*, 2022.
- [29] Z. Chen, S. Meng, F. Yang, L. Shang, and X. Zeng, "Total: Topology optimization of operational amplifier via reinforcement learning," in 2023

- 24th International Symposium on Quality Electronic Design (ISQED). IEEE, 2023, pp. 1–8.
- [30] —, “Macro: Multi-agent reinforcement learning-based cross-layer optimization of operational amplifier,” in *2024 29th Asia and South Pacific Design Automation Conference (ASP-DAC)*. IEEE, 2024, pp. 423–428.
- [31] W. Fang, J. Wang, Y. Lu, S. Liu, Y. Wu, Y. Ma, and Z. Xie, “A survey of circuit foundation model: Foundation ai models for vlsi circuit design and eda,” *arXiv preprint arXiv:2504.03711*, 2025.
- [32] Z. He and B. Yu, “Large language models for eda: Future or mirage?” in *Proceedings of the 2024 International Symposium on Physical Design*, 2024, pp. 65–66.
- [33] Z. Tao, Y. Shi, Y. Huo, R. Ye, Z. Li, L. Huang, C. Wu, N. Bai, Z. Yu, T.-J. Lin *et al.*, “Amsnet: Netlist dataset for ams circuits,” in *2024 IEEE LLM Aided Design Workshop (LAD)*. IEEE, 2024, pp. 1–5.
- [34] Y. Shi, Z. Tao, Y. Gao, T. Zhou, C. Chang, Y. Wang, B. Chen, G. Zhang, A. Liu, Z. Yu *et al.*, “Amsnet-kg: A netlist dataset for llm-based ams circuit auto-design using knowledge graph rag,” *arXiv preprint arXiv:2411.13560*, 2024.
- [35] Y. Hou, J. Zhang, H. Chen, M. Zhou, F. Yu, H. Fan, and Y. Yang, “Cktgen: Specification-conditioned analog circuit generation,” *arXiv preprint arXiv:2410.00995*, 2024.
- [36] Z. Dong, W. Cao, M. Zhang, D. Tao, Y. Chen, and X. Zhang, “Cktgcn: Circuit graph neural network for electronic design automation,” *arXiv preprint arXiv:2308.16406*, 2023.
- [37] Z. Ke, Y. Shao, H. Lin, T. Konishi, G. Kim, and B. Liu, “Continual pre-training of language models,” *arXiv preprint arXiv:2302.03241*, 2023.
- [38] B. Mann, N. Ryder, M. Subbiah, J. Kaplan, P. Dhariwal, A. Neelakantan, P. Shyam, G. Sastry, A. Askell, S. Agarwal *et al.*, “Language models are few-shot learners,” *arXiv preprint arXiv:2005.14165*, vol. 1, 2020.
- [39] C. Li, Z. Yuan, H. Yuan, G. Dong, K. Lu, J. Wu, C. Tan, X. Wang, and C. Zhou, “Mugglemath: Assessing the impact of query and response augmentation on math reasoning,” *arXiv preprint arXiv:2310.05506*, 2023.
- [40] C. Li, W. Wang, J. Hu, Y. Wei, N. Zheng, H. Hu, Z. Zhang, and H. Peng, “Common 7b language models already possess strong math capabilities,” *arXiv preprint arXiv:2403.04706*, 2024.
- [41] W. Zhang, Q. Wang, X. Kong, J. Xiong, S. Ni, D. Cao, B. Niu, M. Chen, Y. Li, R. Zhang *et al.*, “Fine-tuning large language models for chemical text mining,” *Chemical Science*, vol. 15, no. 27, pp. 10600–10611, 2024.
- [42] Y. Shi, Z. Zhang, H. Wang, Z. Tao, Z. Li, B. Chen, Y. Wang, Z. Yu, T.-J. Lin, and L. He, “Amsbench: A comprehensive benchmark for evaluating mllm capabilities in ams circuits,” *arXiv preprint arXiv:2505.24138*, 2025.
- [43] S. Gururangan, A. Marasović, S. Swayamdipta, K. Lo, I. Beltagy, D. Downey, and N. A. Smith, “Don’t stop pretraining: Adapt language models to domains and tasks,” *arXiv preprint arXiv:2004.10964*, 2020.
- [44] H. Touvron, L. Martin, K. Stone, P. Albert, A. Almahairi, Y. Babaei, N. Bashlykov, S. Batra, P. Bhargava, S. Bhosale *et al.*, “Llama 2: Open foundation and fine-tuned chat models,” *arXiv preprint arXiv:2307.09288*, 2023.
- [45] Y. Bai, A. Jones, K. Ndousse, A. Askell, A. Chen, N. DasSarma, D. Drain, S. Fort, D. Ganguli, T. Henighan *et al.*, “Training a helpful and harmless assistant with reinforcement learning from human feedback,” *arXiv preprint arXiv:2204.05862*, 2022.
- [46] C. Zhou, P. Liu, P. Xu, S. Iyer, J. Sun, Y. Mao, X. Ma, A. Efrat, P. Yu, L. Yu *et al.*, “Lima: Less is more for alignment,” *Advances in Neural Information Processing Systems*, vol. 36, pp. 55 006–55 021, 2023.
- [47] Y. Bai, S. Kadavath, S. Kundu, A. Askell, J. Kernion, A. Jones, A. Chen, A. Goldie, A. Mirhoseini, C. McKinnon *et al.*, “Constitutional ai: Harmlessness from ai feedback,” *arXiv preprint arXiv:2212.08073*, 2022.
- [48] R. Rafailov, A. Sharma, E. Mitchell, C. D. Manning, S. Ermon, and C. Finn, “Direct preference optimization: Your language model is secretly a reward model,” *Advances in neural information processing systems*, vol. 36, pp. 53 728–53 741, 2023.
- [49] S. Lin, P. Ju, Y. Liang, and N. Shroff, “Theory on forgetting and generalization of continual learning,” in *International Conference on Machine Learning*. PMLR, 2023, pp. 21 078–21 100.
- [50] Z. Li and D. Hoiem, “Learning without forgetting,” *IEEE transactions on pattern analysis and machine intelligence*, vol. 40, no. 12, pp. 2935–2947, 2017.
- [51] J. Schulman, S. Levine, P. Moritz, M. Jordan, and P. Abbeel, “Trust region policy optimization,” in *Proceedings of the 32nd International Conference on International Conference on Machine Learning - Volume 37*, ser. ICML’15. JMLR.org, 2015, p. 1889–1897.
- [52] J. Rasley, S. Rajbhandari, O. Ruwase, and Y. He, “Deepspeed: System optimizations enable training deep learning models with over 100 billion parameters,” in *Proceedings of the 26th ACM SIGKDD international conference on knowledge discovery & data mining*, 2020, pp. 3505–3506.
- [53] T. Wolf, L. Debut, V. Sanh, J. Chaumond, C. Delangue, A. Moi, P. Cistac, T. Rault, R. Louf, M. Funtowicz, J. Davison, S. Shleifer, P. von Platen, C. Ma, Y. Jernite, J. Plu, C. Xu, T. L. Scao, S. Gugger, M. Drame, Q. Lhoest, and A. M. Rush, “Transformers: State-of-the-art natural language processing,” in *Proceedings of the 2020 Conference on Empirical Methods in Natural Language Processing: System Demonstrations*. Online: Association for Computational Linguistics, Oct. 2020, pp. 38–45. [Online]. Available: <https://www.aclweb.org/anthology/2020.emnlp-demos.6>
- [54] T. Dao, D. Y. Fu, S. Ermon, A. Rudra, and C. Ré, “FlashAttention: Fast and memory-efficient exact attention with IO-awareness,” in *Advances in Neural Information Processing Systems (NeurIPS)*, 2022.
- [55] T. Dao, “FlashAttention-2: Faster attention with better parallelism and work partitioning,” in *International Conference on Learning Representations (ICLR)*, 2024.
- [56] W. Kwon, Z. Li, S. Zhuang, Y. Sheng, L. Zheng, C. H. Yu, J. E. Gonzalez, H. Zhang, and I. Stoica, “Efficient memory management for large language model serving with pagedattention,” in *Proceedings of the ACM SIGOPS 29th Symposium on Operating Systems Principles*, 2023.
- [57] Q. Team, “Qwq-32b: Embracing the power of reinforcement learning,” March 2025. [Online]. Available: <https://qwenlm.github.io/blog/qwq-32b/>
- [58] E. Guha, R. Marten, S. Keh, N. Raoof, G. Smyrnis, H. Bansal, M. Nezhurina, J. Mercat, T. Vu, Z. Sprague, A. Suvarna, B. Feuer, L. Chen, Z. Khan, E. Frankel, S. Grover, C. Choi, N. Muennighoff, S. Su, W. Zhao, J. Yang, S. Pimpalgaonkar, K. Sharma, C. C.-J. Ji, Y. Deng, S. Pratt, V. Ramanujan, J. Saad-Falcon, J. Li, A. Dave, A. Albalak, K. Arora, B. Wulfe, C. Hegde, G. Durrett, S. Oh, M. Bansal, S. Gabriel, A. Grover, K.-W. Chang, V. Shankar, A. Gokaslan, M. A. Merrill, T. Hashimoto, Y. Choi, J. Jitsev, R. Heckel, M. Sathiamoorthy, A. G. Dimakis, and L. Schmidt, “Openthoughts: Data recipes for reasoning models,” 2025. [Online]. Available: <https://arxiv.org/abs/2506.04178>
- [59] K. N. Leung and P. K. Mok, “Analysis of multistage amplifier-frequency compensation,” *IEEE transactions on circuits and systems I: fundamental theory and applications*, vol. 48, no. 9, pp. 1041–1056, 2001.



Zihao Chen received the B.E. degree from the School of Microelectronics at Fudan University, Shanghai, China, in 2021 and is currently pursuing the Ph.D. at the same institution. His research focuses on the cutting-edge technologies like reinforcement learning (RL) and large language models (LLMs), with their applications in electronic design automation (EDA).



Ji Zhuang received the B.E. degree from the School of Microelectronics at Fudan University, Shanghai, China, in 2025 and is currently pursuing the Ph.D. at the same institution. His research interests lie in EDA, with a focus on leveraging LLMs to advance automation in digital front-end design and analog circuit design.



Jinyi Shen received the B.S. degrees in microelectronics from Fudan University, Shanghai, China, in 2021, where he is currently pursuing the Ph.D. degree with the School of Microelectronics. His current research interests include analog circuit design automation and AI for EDA.



Xiaoyue Ke received the B.S. degree in microelectronics from Fudan University, Shanghai, China, in 2024. She is currently working toward the M.S. degree in microelectronics at the same university. Her research interests include analog integrated circuit design, particularly in the area of high-speed SerDes interfaces.



Xinyi Yang received the B.S. degrees in microelectronics from Fudan University, Shanghai, China, in 2025, where she is currently pursuing the Ph.D. degree with the College of Integrated Circuits and Micro-Nano Electronics. Her current research interests include DRC automation and LLM for EDA.



Mingjie Zhou received his high school diploma from Lishui High School, Zhejiang Province, China. He is currently pursuing a bachelor's degree in Microelectronics Science and Engineering at Fudan University, Shanghai, China. His current research focuses on the application of large language models in EDA.



Zhuoyao Du received the B.Eng. degree in Microelectronics Science and Engineering from Fudan University, Shanghai, China in 2025, where he is currently pursuing the M.S. degree. His research focus is hardware accelerator design.



Xu Yan received a bachelor's degree in engineering from Fudan University in 2025 and will continue to study for an academic master's degree in microelectronics. His current research interests is LLM for EDA.



Zhouyang Wu received the B.S. degree from Fudan University in 2025 and is currently pursuing the Ph.D. degree with the School of Microelectronics, Fudan University. Her current research interests include standard cell design and logic synthesis.



Zhenyu Xu received the B.E. degree in Integrated Circuit Design and Integrated Systems from Huazhong University of Science and Technology, Wuhan, China, in 2022. He is currently pursuing the Ph.D. degree with the School of Computer Science, Fudan University, Shanghai, China. His current research interests include intelligent wearable systems and multimodal foundation models.



Jiangli Huang received the B.S. degree in applied physics from the University of Science and Technology of China, Hefei, China, in 2019. He received the Ph.D. degree in microelectronics from Fudan University, Shanghai, China, in 2024. His current research interests include analog circuit design automation and optimization.



Li Shang is a Professor at the School of Computer Science, Fudan University. He received his Ph.D. degree from Princeton University. He was the Deputy Director and Chief Architect of Intel Labs China, and Associate Professor of University Colorado Boulder. His research focuses on embodied intelligence, machine learning, and VLSI & EDA. He has over 170 publications with multiple best paper awards and nominations, and over 8000 citations. He was a recipient of the NSF Career Award.



Xuan Zeng received the B.S. and Ph.D. degrees in electrical engineering from Fudan University, Shanghai, China, in 1991 and 1997, respectively. She is a Full Professor with School of Microelectronics, Fudan University. Her research focuses on analog circuit modeling and synthesis, design for manufacturability, high-speed interconnect analysis and optimization, and circuit simulation. She received the Changjiang Distinguished Professor with the Ministry of Education Department of China in 2014.



Fan Yang received B.S. degree from Xi'an Jiaotong University in 2003 and Ph.D. degree from Fudan University, Shanghai, China, in 2008. He is a Full Professor with the Microelectronics Department in Fudan University. His research interests include model order reduction, circuit simulation, high-level synthesis, acceleration of artificial neural networks, yield analysis and design for manufacturability.